INTERNATIONAL STANDARD

ISO 23365

First edition
2022-07

Heavy commercial vehicles and buses — Definitions of properties for the determination of suspension kinematic and compliance characteristics

Véhicules utilitaires lourds et autobus — Définitions des propriétés pour la détermination des caractéristiques cinématiques et de conformité des suspensions

Reference number
ISO 23365:2022(E)

ISO copyright office
CP 401 • Ch. de Blandonnet 8
CH-1214 Vernier, Geneva
Phone: +41 22 749 01 11
Email: copyright@iso.org
Website: www.iso.org

Published in Switzerland

Contents

Page

Foreword

ISO (the International Organization for Standardization) is a worldwide federation of national standards bodies (ISO member bodies). The work of preparing International Standards is normally carried out through ISO technical committees. Each member body interested in a subject for which a technical committee has been established has the right to be represented on that committee. International organizations, governmental and non-governmental, in liaison with ISO, also take part in the work. ISO collaborates closely with the International Electrotechnical Commission (IEC) on all matters of electrotechnical standardization.

The procedures used to develop this document and those intended for its further maintenance are described in the ISO/IEC Directives, Part 1. In particular, the different approval criteria needed for the different types of ISO documents should be noted. This document was drafted in accordance with the editorial rules of the ISO/IEC Directives, Part 2 (see www.iso.org/directives).

Attention is drawn to the possibility that some of the elements of this document may be the subject of patent rights. ISO shall not be held responsible for identifying any or all such patent rights. Details of any patent rights identified during the development of the document will be in the Introduction and/or on the ISO list of patent declarations received (see www.iso.org/patents).

Any trade name used in this document is information given for the convenience of users and does not constitute an endorsement.

For an explanation of the voluntary nature of standards, the meaning of ISO specific terms and expressions related to conformity assessment, as well as information about ISO's adherence to the World Trade Organization (WTO) principles in the Technical Barriers to Trade (TBT), see www.iso.org/iso/foreword.html.

This document was prepared by Technical Committee ISO/TC 22, *Road vehicles*, Subcommittee SC 33, *Vehicle dynamics and chassis components*.

Any feedback or questions on this document should be directed to the user's national standards body. A complete listing of these bodies can be found at www.iso.org/members.html.

Introduction

The dynamic behaviour of a road vehicle is a very important aspect of active vehicle safety. Any given vehicle, together with its driver and the prevailing environment, constitutes a closed-loop system that is unique. The task of evaluating the dynamic behaviour is therefore, very difficult since the significant interaction of these driver-vehicle-environment elements are each complex in themselves. A complete and accurate description of the behaviour of the road vehicle shall necessarily involve information obtained from a number of different tests.

Static properties of the vehicle and its systems can have an important impact on the vehicle dynamic behaviour and a driver's or automation's ability to generate the desired motion. Test conditions have a strong influence on test results. Therefore, only vehicle dynamic and static properties obtained under virtually identical test conditions are comparable to one another.

Since this test method quantifies only one small part of the complete vehicle handling characteristics, the results of these tests can only be considered significant for a correspondingly small part of the overall dynamic behaviour.

Moreover, insufficient knowledge is available concerning the relationship between overall vehicle dynamic properties and accident avoidance. A substantial amount of work is necessary to acquire sufficient and reliable data on the correlation between accident avoidance and vehicle dynamic properties in general and the results of these tests in particular. Consequently, it is important for any application of this test method for regulation purposes the proven correlation between test results and accident statistics.

Heavy commercial vehicles and buses — Definitions of properties for the determination of suspension kinematic and compliance characteristics

1 Scope

This document applies to heavy vehicles—that is, to commercial vehicles and buses as defined in ISO 3833—that are covered by the categories M3, N2, N3, O3, and O4 of ECE and EC vehicle regulations. These categories pertain to trucks and trailers with maximum weights above 3,5 tonnes and to buses with maximum weights above 5 tonnes.

Vehicle suspension kinematic and compliance (K&C) properties that impact vehicle stability and dynamic behaviour are described in this document and common methods of measurement are outlined. These methods are applicable to heavy vehicles. The measurements are performed on a single unit and typically one or two axles at a time.

This document will define or reference the key suspension kinematic and compliance parameters necessary for characterizing and simulating vehicle suspension performance. These parameters also provide system-level descriptions of quasi-static behaviour that can be cascaded into subsystem and component performance targets. The suspension variables required for determining suspension characterization of one vehicle end, i.e. for a single axle or for multiple axles inter-related through suspension configuration (for example, walking-beam), are provided. Metrics pertaining to the chassis connection between the front and rear suspensions are not included. Some typical methods of measurement will be discussed, however detail on how the measurements are executed is not within the scope of this document.

2 Normative references

The following documents are referred to in the text in such a way that some or all of their content constitutes requirements of this document. For dated references, only the edition cited applies. For undated references, the latest edition of the referenced document (including any amendments) applies.

ISO 8855, *Road vehicles — Vehicle dynamics and road-holding ability — Vocabulary*

ISO 15037-2, *Road vehicles — Vehicle dynamics test methods — Part 2: General conditions for heavy vehicles and buses*

3 Terms and definitions

For the purposes of this document, the terms and definitions given in ISO 8855, ISO 15037-2 and the following apply.

ISO and IEC maintain terminology databases for use in standardization at the following addresses:

— ISO Online browsing platform: available at https://www.iso.org/obp

— IEC Electropedia: available at https://www.electropedia.org/

3.1
side view swing centre
point in a plane parallel to the X_V-Z_V plane that intersects the wheel centre and locates the instantaneous centre of rotation of the wheel centre resulting from a displacement in the Z_V direction

3.2
side view swing arm angle
angle from a horizontal line parallel to the X_V-Z_V plane that intersects the *side view swing centre* (3.1) and the line that intersects the side view swing centre and wheel centre

3.3
longitudinal force compliance, with suspension torque
$x_{\vec{F}_X}'$
rate of change of the wheel centre displacement in the X_V direction with respect to a force exerted on the geometric centre of the tyre contact patch in the X_V direction

3.4
longitudinal force compliance, without suspension torque
$x_{\vec{F}_{XW}}'$
rate of change of the wheel centre displacement in the X_V direction with respect to a force exerted on the wheel centre in the X_V direction

3.5
longitudinal force camber compliance, with suspension torque
$\varepsilon_{V\vec{F}_X}'$
rate of change of camber angle with respect to a force exerted on the geometric centre of the tyre contact patch in the X_V direction

3.6
longitudinal force camber compliance, without suspension torque
$\varepsilon_{V\vec{F}_{XW}}'$
rate of change of camber angle with respect to a force exerted on the wheel centre in the X_V direction

3.7
longitudinal force steer compliance, with suspension torque
$\delta_{\vec{F}_X}'$
rate of change of steer angle with respect to a force exerted on the geometric centre of the tyre contact patch in the X_V direction

3.8
longitudinal force steer compliance, without suspension torque
$\delta_{\vec{F}_{XW}}'$
rate of change of steer angle with respect to a force exerted on the wheel centre in the X_V direction

3.9
longitudinal force windup compliance, with suspension torque
$\tau_{\vec{F}_X}'$
rate of change of the axle or hub assembly angle about the Y_V axis with respect to a force exerted on the geometric centre of the tyre contact patch in the X_V direction

3.10
longitudinal force windup compliance, without suspension torque
$\tau_{\vec{F}_{XW}}'$
rate of change of the axle or hub assembly angle about the Y_V axis with respect to a force exerted on the wheel centre in the X_V direction

3.11
lateral force compliance at the wheel centre
$y_{\vec{F}_{YW}}{}'$
rate of change of wheel centre displacement in the Y_V direction with respect to a force exerted on the geometric centre of the tyre contact patch in the Y_V direction

3.12
lateral force compliance at the contact centre
$y_{\vec{F}_Y}{}'$
rate of change of geometric centre of the tyre contact patch displacement in the Y_V direction with respect to a force exerted on the geometric centre of the tyre contact patch in the Y_V direction

3.13
lateral force camber compliance
$\varepsilon_{V\vec{F}_Y}{}'$
rate of change of camber angle with respect to a force exerted on the geometric centre of the tyre contact patch in the Y_V direction

3.14
lateral force steer compliance
$\delta_{\vec{F}_Y}{}'$
rate of change of steer angle with respect to a force exerted on the geometric centre of the tyre contact patch in the Y_V direction

3.15
aligning moment camber compliance
$\varepsilon_{V\vec{M}_Z}{}'$
rate of change of camber angle with respect to a moment exerted on the tyre contact patch about the Z_V axis

3.16
aligning moment steer compliance
$\delta_{\vec{M}_Z}{}'$
rate of change of steer angle with respect to a moment exerted on the tyre contact patch about the Z_V axis

3.17
auxiliary roll stiffness
$K_{\varphi_V,aux}$
contribution to roll stiffness beyond that which results from ride rate and symmetric vertical tyre contact patch-to-body displacement

3.18
auxiliary suspension roll stiffness
$K_{\varphi_K,aux}$
contribution to suspension roll stiffness beyond that which results from suspension ride rate and symmetric vertical wheel-to-body displacement

3.19
total ride toe
$\delta_{z(R-L)}$
change in the difference of the left steer angle from the right steer angle observed in *ride mode* (3.22)

3.20
total ride toe gradient
$\delta_{z(R\text{-}L)}'$
differential of *total ride toe* (3.19) with suspension travel as observed in *ride mode* (3.22)

3.21
wheel pad
surface of the kinematic and compliance measurement facility that supports each tyre contact patch and is typically capable of applying forces at the geometric centre of the tyre contact patch in the *X* and *Y* directions, moments at the tyre contact patch about the *Z* axis, and optionally displacements in the *Z* direction

Note 1 to entry: The wheel pads are assumed to represent the ground plane. If the vehicle sprung mass is not rolled relative to the wheel pads, it can be assumed that the intermediate axis system and vehicle axis system coincide.

3.22
ride mode
motion of vehicle suspension produced by near-equal Z_T displacements of the wheel centres on a single axle relative to the vehicle body, with *wheel pad* (3.21) *X* and *Y* forces and Z_T moments controlled to as near-zero as practicable, and preferably with the change in $\vec{M}_X$ held as near to zero as practicable

3.23
roll mode
motion of single axle produced by a pure roll moment, $\vec{M}_X$, resulting from equal and opposite change in the forces applied to the left and right tyre contact centres of each axle in the Z_T direction, with *wheel pad* (3.21) *X* and *Y* forces and Z_T moments controlled to as near-zero as practicable

4 Principle

This document defines the common suspension kinematic and compliance (K&C) properties of suspensions that relate to the change in orientation of the road wheel and tyre to the road surface as a result of, and relative to, forces, moments and displacements input to the tyre contact patches. The forces, moments and displacements are intended to reflect those encountered in real-world manoeuvres. Characterization of these properties is essential to modelling the ride and handling behaviour of road vehicles as the motion of the tyre contact patch relative to the sprung mass is determined by both the sprung mass to tyre orientation and the tyre to road surface orientation.

The intent of K&C measurements is to isolate the change in ground and wheel planes to vehicle sprung mass orientation that result from each of the relevant primary forces, moments and displacements. For instance, lateral force steer compliance is measured by suppressing other inputs that steer angle is sensitive to, such as change in longitudinal force or steer moment. The lateral force steer compliance is isolated by controlling the wheel pad longitudinal force and steer moment to zero and constraining the vertical position of the contact patch to avoid introducing kinematic effects resulting from trim height change. Similarly, other measurements are made with constraints defined to isolate the change resulting from particular forces, moments or displacements to facilitate the principle of superposition when used in a vehicle simulation.

While it is essential to isolate the reactions to specific forces, moments or displacements, the inputs shall be representative of naturally occurring inputs. For example, when measuring the roll characteristics of a suspension, it is strongly preferred to simulate the sprung mass roll relative the ground plane. This may be achieved using asymmetric vertical displacement of the wheel pads or by rolling the vehicle body relative to the wheel pads. In either case, the sum of the normal forces exerted on the axle shall remain constant. This is more representative of on-road behaviour than the input of equal and opposite vertical displacements at the tyre contact patches.

5 Variables

5.1 Reference system

Variables used to characterize vehicle suspension K&C properties are typically determined in the following manner:

— the change in wheel orientation as defined by the wheel axis system (X_W, Y_W, Z_W) resulting from a displacement, force, or moment aligned to the intermediate axis system (X, Y, Z) (see ISO 8855);

— the displacement of the wheel centre as defined by the intermediate coordinate system (x, y, z) resulting from a force aligned to the intermediate axis system (X, Y, Z) (see ISO 8855);

— the change in vehicle sprung mass orientation as defined by the vehicle axis system (X_V, Y_V, Z_V) resulting from a displacement, force, or moment aligned to the intermediate axis system (X, Y, Z) (see ISO 8855).

NOTE Ideally the changes in wheel orientation due to tyre forces and moments would be determined relative to the tyre forces and moments in the tyre axis system (X_T, Y_T, Z_T), since this is the reference system in which tyre force and moment properties are provided. However, it typically is not practical to maintain contact patch shear force alignment with the tyre axis system in a K&C machine and so, the shear forces are normally aligned with the intermediate axis system. For the small angles that normally result during compliance measurements, the differences can be neglected.

5.2 Variables to be determined

Variable definitions not found in ISO 8855 can be found in Clause 3. To describe the relative suspension motions resulting from external forces and moments, the principal relevant variables are the following:

5.2.1 Vehicle geometry

— wheel centre

— contact centre

— contact patch

— tandem axle spacing

— b, track

5.2.2 Motion variables

— φ_V, vehicle roll angle

— φ_K, suspension roll angle

— ride displacement

— bogie orientation variables (pitch, roll, twist)

5.2.3 Forces and moments

— $\vec{F}_X$, longitudinal force

— $\vec{F}_Y$, lateral force

— $\vec{F}_Z$, vertical force

— $\vec{M}_X$, roll moment

— $\vec{M}_S$, steering-axis torque

— $\vec{F}_{XT}$, tyre longitudinal force at the contact centre

— $\vec{F}_{YT}$, tyre lateral force at the contact centre

— $\vec{F}_{ZT}$, tyre vertical force at the contact centre

— $\vec{F}_{XW}$, longitudinal force at the wheel centre

5.2.4 Steering geometry

— δ, steer angle

— δ_{kin}, kinematic steer angle

— $\delta_{m,kin}$, mean kinematic steer angle

— $\delta_{inc,kin}$, included kinematic steer angle

— static toe angle

— total static toe angle

— δ_H, steering wheel angle

— Ackermann error

— steering ratio

— i_S, overall steering ratio

— ε_W, inclination angle (actual measurement)

— ε_V, camber angle (calculated)

— τ, castor angle

— n_k, castor offset at ground

— n_τ, castor offset at wheel centre

— δ_m, mean steer angle

— σ, steering-axis inclination angle

— r_K, steering-axis offset at ground

— r_σ, steering-axis offset at wheel centre

— r, scrub radius

5.2.5 Kinematics

— b_z, ride track change

— b_z', ride track change gradient

— δ_z, ride steer

— δ_z', ride steer gradient

— ε_{Vz}, ride camber

— ε_{Vz}', ride camber gradient

— τ_z, ride castor

— τ_z', ride castor gradient

— $\delta_{\varphi V}$, roll steer

— $\delta_{\varphi V}'$, roll steer gradient

— $\varepsilon_{V\varphi V}$, roll camber

— $\varepsilon_{V\varphi V}'$, roll camber gradient

— $\tau_{\varphi V}$, roll castor

— $\tau_{\varphi V}'$, roll castor gradient

— roll centre height

— side view swing arm angle

5.2.6 Compliances

— $x_{\vec{F}X}'$, longitudinal force compliance, with suspension torque

— $x_{\vec{F}XW}'$, longitudinal force compliance, without suspension torque

— $\varepsilon_{V\vec{F}X}'$, longitudinal force camber compliance, with suspension torque

— $\varepsilon_{V\vec{F}XW}'$, longitudinal force camber compliance, without suspension torque

— $\delta_{\vec{F}X}'$, longitudinal force steer compliance, with suspension torque

— $\delta_{\vec{F}XW}'$, longitudinal force steer compliance, without suspension torque

— $\tau_{\vec{F}X}'$, longitudinal force windup compliance, with suspension torque

— $\tau_{\vec{F}XW}'$, longitudinal force windup compliance, without suspension torque

— $y_{\vec{F}Y}'$, lateral force compliance at the contact centre

— $y_{\vec{F}YW}'$, lateral force compliance at the wheel centre

— $\varepsilon_{V\vec{F}Y}'$, lateral force camber compliance

— $\delta_{\vec{F}Y}'$, lateral force steer compliance

— $\varepsilon_{V\vec{M}Z}'$, aligning moment camber compliance

— $\delta_{\vec{M}Z}'$, aligning moment steer compliance

5.2.7 Ride and roll stiffness

— K_Z, ride rate

— K_{ZK}, suspension ride rate

— $K_{\varphi V}$, roll stiffness

— $K_{\varphi K}$, suspension roll stiffness

— $K_{\varphi V,aux}$, auxiliary roll stiffness

— $K_{\varphi K,aux}$, auxiliary suspension roll stiffness

— K_{tz}, vertical displacement tandem axle load redistribution stiffness

— K_{tzK}, vertical suspension displacement tandem axle load redistribution stiffness

— $K_{\varphi t}$, tandem axle twist stiffness

— $K_{\varphi tK}$, tandem axle suspension twist stiffness

— K_{ZT}, tyre normal stiffness

5.2.8 Force reactions

— $\vec{F}_{Z\vec{F}_X}{}'$, anti-squat and anti-dive force gradient

— $\vec{F}_{Z\vec{F}_Y}{}'$, jacking force gradient

— $W_{Dt\vec{F}_{XT}}{}'$, longitudinal force tandem axle dynamic load transfer

6 Measuring equipment

6.1 Measurement accuracy

Variables measured to characterize vehicle suspension kinematic and compliance properties are presented in Table 1. Typical operating ranges are presented, as well as minimum accuracy recommendations. Either accuracy (percentage of full scale or absolute) may be used. Several references are made throughout this document to holding forces or moments to "as near-zero as practicable" to minimize their influence on a particular measurement. The values presented in the "near-zero threshold" column represent the recommended maximum controlled and measured value for such forces or moments.

Table 1 — Variables to be measured

Variable [a]	Typical operating range	Accuracy (% of full scale)	Absolute accuracy	Near-zero threshold
ε_W, inclination angle	±10°	±1,0	0,1°	
τ, castor angle	±10°	±1,0	0,1°	
δ, steer angle (K&C test)	±5°	±2,0	0,1°	
δ_{kin}, kinematic steer angle (steering ratio test)	±45°	±0,2	0,1°	
δ_H, steering-wheel angle (steering ratio test)	±1 080°	±0,1	1,0°	
suspension longitudinal displacement	±100 mm	±1,0	1,0 mm	
suspension lateral displacement	±100 mm	±1,0	1,0 mm	
suspension ride displacement	±150 mm	±0,7	1,0 mm	
ride displacement	±200 mm	±0,25	0,4 mm	
φ_K, suspension roll angle	±4°	±1,5	0,06°	
φ_V, vehicle roll angle	±5°	±0,6	0,03°	

Table 1 *(continued)*

Variable [a]	Typical operating range	Accuracy (% of full scale)	Absolute accuracy	Near-zero threshold
$\vec{M}_{ZT}$, tyre aligning moment	±4 000 N·m	±0,25	10,0 N·m	20 N·m
$\vec{F}_{XT}$, tyre longitudinal force at contact centre	±30 000 N	±0,25	75 N	100 N
$\vec{F}_{YT}$, tyre lateral force at contact centre	±30 000 N	±0,25	75 N	100 N
$\vec{F}_{ZT}$, tyre normal force at contact centre	(60 000±60 000) N	±0,2	120 N	100 N
$\vec{F}_{XW}$, longitudinal force at wheel centre	±30 000 N	±0,25	75 N	100 N

6.2 Derived variable accuracy

Variables calculated to characterize vehicle suspension kinematic and compliance properties are presented in Table 2.

Table 2 — Derived variables

Variable [a]	Typical operating range	Accuracy (% of full scale)	Absolute accuracy
i_S, overall steering ratio	15 to 30	±1,5	0,5
$\varepsilon_{V\vec{M}_Z}'$, aligning moment camber compliance	(-1,5 to 2,5)°/kNm	±10,0	0,25°/kNm
$\delta_{\vec{M}_Z}'$, aligning moment steer compliance	(0 to 0,5)°/kNm	±5,0	°/kNm
$\varepsilon_{V\vec{F}_Y}'$, lateral force camber compliance	(-2,5 to 2,5)°/kN	±5,0	0,1°/kN
$y_{\vec{F}_Y}'$, lateral force compliance at the contact centre	(0,005 to 10,0) mm/kN	±5,0	mm/kN
$\delta_{\vec{F}_Y}'$, lateral force steer compliance	(-0,05 to 2,0)°/kN	±5,0	
$K_{\varphi K}$ suspension roll rate	(500 to 40 000) Nm/°	±5,0	
K_{ZK}, suspension ride rate	(11 to 2 400) N/mm	±5,0	
ε_{Vz}', ride camber gradient	(-0,1 to 0,1)°/mm	±2,0	±0,02°/mm
τ_Z', ride castor gradient	(-0,05 to 0,05)°/mm	±10,0	±0,02°/mm
δ_z', ride steer gradient	(-0,15 to 0,15)°/mm	±2,0	±0,000 4°/mm
$\varepsilon_{V\varphi_V}'$, roll camber gradient	(0 to 1)°/°	±2,0	±0,01°/°
$\tau_{\varphi V}'$, roll castor gradient	(0 to 0,5)°/°	±10,0	±1,0 %
roll centre height	(-100 to 1,000) mm	±2,5	±2,5 mm
$\delta_{\varphi V}'$, roll steer gradient	(-0,25 to 0,25)°/°	±2,0	±0,25 %

7 Suspension parameter measurement guidance

7.1 Steering geometry

7.1.1 Steering ratio

Steering ratio, defined in ISO 8855, is the rate of change of steering-wheel angle with respect to the mean kinematic steer angle at a given steering-wheel angle. Testing is conducted by the simultaneous

measurement of steering-wheel angle and the left and right kinematic steer angles as the steering-wheel is turned throughout its range of motion. Mean kinematic steer angle is determined by averaging the coincident individual kinematic steer angles on the axle for calculation of the steering ratio. In practice, the wheel pad vertical position is held fixed relative to the vehicle body as the steering-wheel is turned at a slow smooth rate, on the order of one turn per minute with any available power assist activated. Forces in the *X*-*Y* plane and moments about the Z_T axes are controlled to as near-zero as practicable.

It is recommended that a minimum of three continuous lock-to-lock steer cycles be completed for analysis. The straight ahead steering-wheel angle position is best determined by driving the vehicle straight ahead and noting the position of the steering-wheel prior to making K&C measurements. This position should be defined as zero. Alternatively, if absolute steer angles are measured, zero steering-wheel angle can be defined where the mean steer angle is zero. Although the steering ratio test can commence from the straight-ahead steering-wheel position, smoothing and/or curve fitting of the data may be performed better when the test commences from the steering-wheel angle turned full clockwise or counter-clockwise to avoid the discontinuity in the data occurring near-zero steering-wheel angle.

One recommended method of characterizing steering ratio as a function of steering-wheel angle is to fit a formula to the data. It is recommended that the steering-wheel angle and left and right steer angle data be smoothed prior to calculating steering ratio. A moving mean filter works adequately as long as there are sufficient data points beyond the range over which the ratio is to be calculated. A sample plot of left and right steer angles versus steering-wheel angle is shown in Clause 8. A moving mean filter will result in truncation of several initial and final data points in the time-history data traces. After smoothing, point-to-point or other numerical differentials can be taken to calculate steering ratios for the left, right, and mean steer angles. Curve fits can be applied to the cross plot of steering ratio for left, right, and mean kinematic steer angle versus steering-wheel angle.

The steering gear, steering linkage geometry, and steering shaft joints contribute to nonlinearities in the relationship between steering ratio and steering-wheel angle. Although it is possible to fit a polynomial curve or Fourier series to this relationship, a more specialised fit should be considered. Basic steering ratio may include first-order and second-order polynomial terms to represent asymmetry and curvature. Typical steering shaft universal joint phasing anomalies may be represented by including a scaled sinusoidal term having a period of two cycles per steering-wheel revolution. Minimizing the squared difference between the ratio calculated from the raw data and the curve fit formula results will provide the values for the coefficients. The term values determined from the curve fits can be used to characterize the various steering ratio properties. If individual left and right steering ratio curve fits are determined, they can be used to provide continuous smooth data for calculating properties such as Ackermann error or turn diameter as a function of steering-wheel angle. An example cross plot of steering-wheel angle and the left and right kinematic steer angles and curve fits for left wheel, right wheel, and overall steering ratio versus steering-wheel angle are shown in Clause 8.

NOTE 1 A unique steering ratio can be measured for each steerable axle of a multi-steered axle vehicle. However, electronically controlled steering systems that change steering ratio with vehicle speed or other state variable are only valid for the state in which the test is performed.

NOTE 2 Although kinematic steer angle is defined as the road wheel steer angle resulting from a steering-wheel angle with the vertical wheel-to-body distance fixed, for practical measurement purposes, the vertical wheel-to-body travel need not be constrained. Tyre deflection resulting from steering axes that are not normal to the wheel pads and the offsets in geometric centres of the tyre contact patch can result in wheel centres being displaced relative to the vehicle body and a net steering system moment. The subsequent steer resulting from suspension geometry and steering compliance is much smaller than that caused by steering system geometry and is typically ignored.

7.1.2 Overall steering ratio (i_S)

Overall steering ratio is defined in ISO 8855. Vehicles that have more than one steer axle will require that the steering ratio measurements for the individual steer axles be used to determine the relationship of steering-wheel angle with respect to the included kinematic steer angle as defined in ISO 8855.

7.1.3 Ackermann error

Ackermann error, defined in ISO 8855, is determined as a function of steering-wheel angle from data collected in a steering ratio test. The left and right kinematic steer angle to steering-wheel angle relationships can be determined by smoothing the raw data and/or by employing curve fits in a manner similar to that discussed for steering ratio. ISO 8855 provides the definition for Ackermann error for single or multi-steer axle systems. It is also possible to calculate the theoretical radius of turn, R, for the vehicle based upon the geometric relationship between the included kinematic steer angle, $\delta_{\text{inc,kin}}$ and the vehicle wheelbase, l, according to Formula (1):

$$R = \frac{l}{\delta_{\text{inc,kin}}} \tag{1}$$

An example of the relationship of Ackermann error and theoretical radius of turn versus steering-wheel angle for a single steer axle vehicle is shown in Clause 8.

7.1.4 Inclination angle (ε_W)

Inclination angle, defined in ISO 8855, is the angle from the Z_T axis and the Z_W axis, in other words, the angle the wheel plane makes with a line perpendicular to the road plane, about the X_V axis. Like steer angle, inclination angle is a direct absolute measurement, however it is relative to the ground plane and not the vehicle body.

7.1.5 Camber angle (ε_V)

Camber angle, defined in ISO 8855, is the angle between the Z_V axis and the wheel plane, about the X_V axis. Like steer angle, camber angle is a direct absolute measurement relative to the vehicle body.

7.1.6 Castor angle (τ)

Castor angle (Figure 1), defined in ISO 8855, can be determined from data collected in a steering ratio test. As steer angle changes, the wheel and hub assembly rotates in front view as a result of castor angle, which is observed as a change in camber angle. For small steer angle change about straight-ahead, castor angle can be calculated from the relationship of the measurement of the change in camber angle with steer angle from Formula (2):

$$\tau = \sin^{-1}\left(\frac{\partial \varepsilon_V}{\partial \delta}\right) \tag{2}$$

Where castor angle is in radians and the differential is taken at zero mean kinematic steer angle.

7.1.7 Castor offset at ground (n_k)

Castor offset at the ground (Figure 1), defined in ISO 8855, can be determined from data collected in a steering ratio test. Also referred to as castor trail or kinematic trail, castor offset at the ground is the longitudinal distance (parallel to the X_T axis) from the tyre contact centre to point of intersection of the steering axis with the road plane. As steer angle changes, the wheel and hub assembly rotates in top view and the tyre contact centre rotates about the point of intersection of the steering axis with the road plane, within in the road plane. For small steer angle change about straight-ahead, the castor offset at the ground can be calculated from Formula (3):

$$n_k = \frac{180}{\pi}\left(\frac{\partial y_T}{\partial \delta}\right) \tag{3}$$

Where y_T is the displacement of the tyre contact centre in the Y_T direction as steer angle, δ, changes.

NOTE If determination of the tyre contact centre displacement is not practical, measurement of the displacement of the wheel pad in the Y_T direction is accepted as sufficient especially for small steer angle changes.

7.1.8 Castor offset at wheel centre (n_τ)

Castor offset at wheel centre (Figure 1), defined in ISO 8855, can be determined from data collected in a steering ratio test. Also referred to as spindle trail, castor offset at wheel centre is the distance measured in the X_T direction between the projection of the wheel centre and the projection of the steering axis on to the X_T-Z_T plane. This measurement is positive if the projection of the steering axis is forward of the projection of the wheel centre. As steer angle changes, the wheel and hub assembly rotates in top view and the wheel centre rotates about the steering axis. For small steer angle change about straight-ahead, the castor offset at wheel centre can be calculated from Formula (4):

$$n_\tau = \frac{180}{\pi}\left(\frac{\partial y_W}{\partial \delta}\right) \tag{4}$$

Where y_W is the displacement of the wheel centre in the Y_W direction as steer angle, δ, changes.

7.1.9 Steering-axis inclination angle (σ)

Steering-axis inclination angle (Figure 1), defined in ISO 8855 can be determined from data collected in a steering ratio test. Also referred to as kingpin inclination angle, steering-axis inclination angle is the angle between the Z_V axis and the normal projection of the steering axis on to the Y_V-Z_V plane. This measurement is positive when the top of the steering axis is inclined inward. As steer angle changes, the wheel and hub assembly rotates in side view as a result of steering-axis inclination, which is observed as a change in castor angle. For small steer angle change about straight-ahead, steering axis inclination angle can be calculated from the relationship of the measured change in castor angle with steer angle from Formula (5):

$$\sigma = \sin^{-1}\left(\frac{\partial \tau}{\partial \delta}\right) \tag{5}$$

Where steering-axis inclination angle is in radians.

7.1.10 Steering-axis offset at ground (r_k)

Steering-axis offset at ground (Figure 1), defined in ISO 8855, can be determined from data collected in a steering ratio test. Also referred to as kingpin offset at ground, steering-axis offset at ground is the lateral distance (measured along the Y_T axis) between the wheel plane (X_W-Z_W plane) and the point where the steering axis intersects the with the road plane (X_T-Y_T plane). As steer angle changes, the wheel and hub assembly rotates in top view and the tyre contact centre rotates about the point of intersection of the steering axis with the road plane, within in the road plane. For small steer angle change about straight-ahead, the castor offset at the ground can be calculated from Formula (6):

$$r_k = \frac{180}{\pi}\left(\frac{\partial x_T}{\partial \delta}\right) \tag{6}$$

Where x_T is the displacement of the tyre contact centre in the X_T direction as steer angle, δ, changes.

NOTE If determination of the tyre contact centre displacement is not practical, measurement of the displacement of the wheel pad in the X_T direction is accepted as sufficient especially for small steer angle changes.

7.1.11 Steering-axis offset at wheel centre (r_σ)

Steering-axis offset at wheel centre (Figure 1), defined in ISO 8855, can be determined from data collected in a steering ratio test. Also referred to as kingpin offset at wheel centre, steering-axis offset at wheel centre is the distance in the Y_T direction between the wheel centre and the projection of the steering axis on to the Y_W-Z_W plane. This measurement is positive if the projection of the steering axis is inboard of the wheel centre. As steer angle changes, the wheel and hub assembly rotates in top view

and the wheel centre rotates about the steering axis. For a small steer angle change about straight-ahead, the steering-axis offset at wheel centre can be calculated from Formula (7):

$$r_\sigma = \frac{180}{\pi}\left(\frac{\partial x_W}{\partial \delta}\right) \tag{7}$$

Where x_W is the displacement of the wheel centre in the X_W direction as steer angle, δ, changes.

7.1.12 Normal steering-axis offset at ground (q_T)

Normal steering-axis offset at ground (Figure 1), defined in ISO 8855, can be determined from data collected in a steering ratio test. Normal steering-axis offset at ground is the normal distance from the contact centre to the projection of the steering axis on to the Y_T-Z_T plane. This measurement is positive if the projection of the steering axis is inboard of the wheel centre. The normal steering axis offset at ground can be calculated from Formula (8):

$$q_T = r_k \cos(\sigma) \tag{8}$$

7.1.13 Normal steering axis offset at wheel centre (q_W)

Normal steering axis offset at wheel centre (Figure 1), defined in ISO 8855, can be determined from data collected in a steering ratio test. Normal steering axis offset at wheel centre is the normal distance from the wheel centre to the projection of the steering axis on to the Y_W-Z_W plane. This measurement is positive if the projection of the steering axis is inboard of the wheel centre. The normal steering axis offset at wheel centre can be calculated from Formula (9):

$$q_W = r_\sigma \cos(\sigma) \tag{9}$$

7.1.14 Scrub radius (r)

Scrub radius (Figure 1), defined in ISO 8855, can be determined from data collected in a steering ratio test. Scrub radius is the distance from the tyre contact centre and the point of intersection of the steering axis and the road plane. As steer angle changes, the tyre contact centre rotates about the steering axis. For a small steer angle change about straight-ahead, scrub radius can be calculated from this relationship as in Formula (10):

$$r = \frac{180}{\pi}\left(\frac{\sqrt{\partial x_T^2 + \partial y_T^2}}{\partial \delta}\right) \tag{10}$$

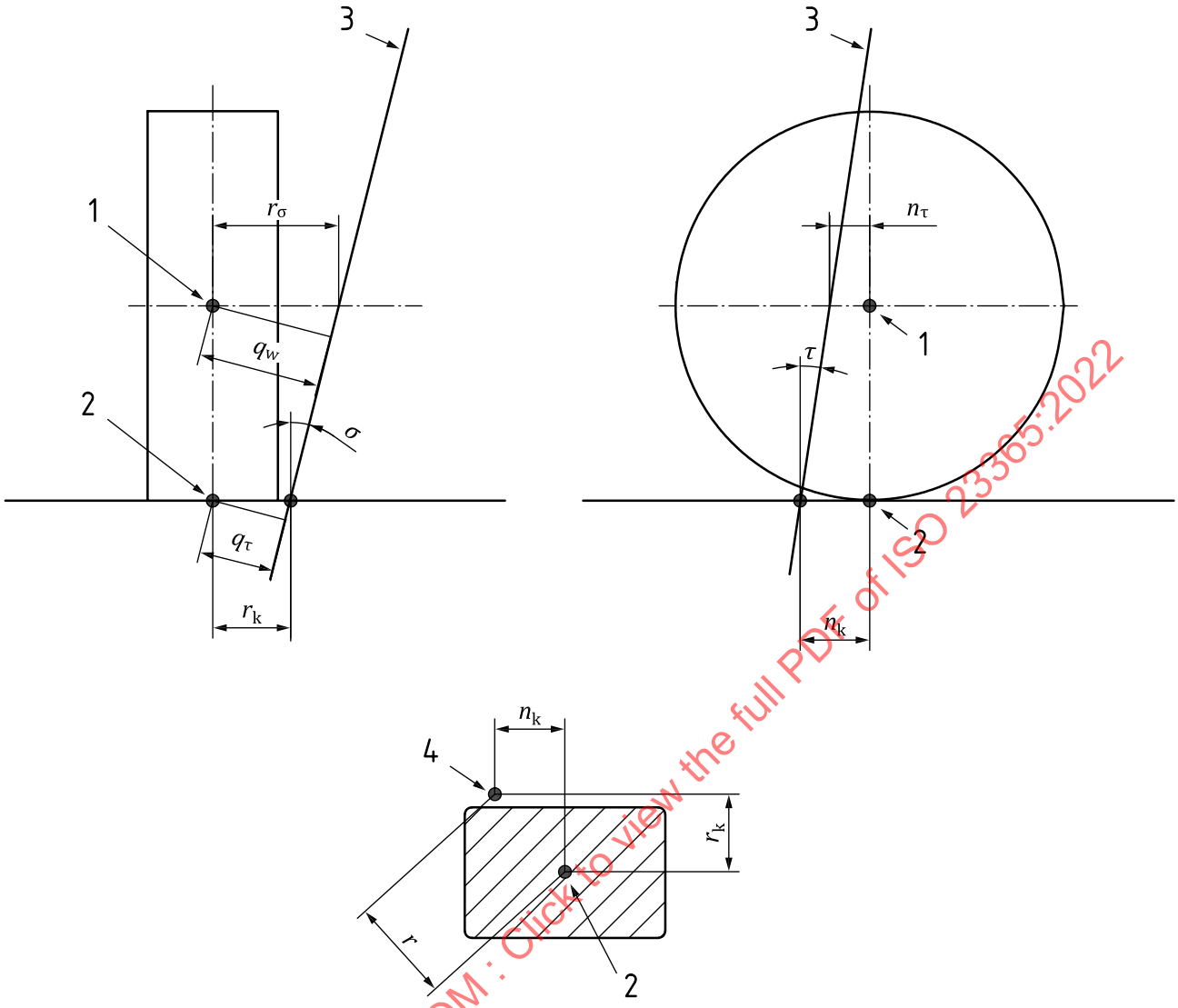

Key

1 wheel centre
2 contact centre
3 steering axis
4 intersection of steering axis with the road plane

Figure 1 — Steering-axis geometry (from ISO 8855)

7.2 Kinematics

7.2.1 General

Suspension kinematic characteristics are typically measurements that result from ride and roll displacements of the suspension. Ride mode is ideally characterized by near-equal vertical displacements of the wheel centres on a single axle. Roll mode is ideally characterized by a pure roll moment input to the vehicle through equal and opposite forces applied to the left and right tyre contact centres of each axle in the Z_T direction. For a steer axle, it is necessary that any available power assist be activated for both the ride mode and roll mode. In ride mode, any asymmetry in steering axis geometry may result in a net moment about the kingpin, which the power assist will act to resist. Alternatively, the steering gear may be locked so as to make the steering as rigid as possible to measure the kinematic ride mode properties. Likewise, in roll mode, the power assist will act to resist the steering moment

introduced by asymmetric vertical forces introduced to roll the suspension. In this case, it is advisable that the steering system not be locked so as to observe the effect of steering system compliance on the kinematic roll properties of the suspension.

In the ride mode, both wheel pads on the same axle are equally displaced vertically relative to the vehicle body. Alternatively, left and right wheel pad displacement should be in force control with $\vec{M}_Z$ held as near to zero as practicable. With either method, wheel pad X_T and Y_T forces and Z_T moments are controlled to as near-zero as practicable. Although equal wheel centre vertical displacements are desirable for determining suspension characteristics relative to the wheel centre, typically the difference in left to right wheel centre displacements is negligible for equal tyre contact patch displacements. Typical differences result from unequal tyre normal stiffnesses due to unequal tyre pressure, or from unequal suspension ride rates due to production variation resulting in asymmetric spring rates, bushing rates, or geometry. To the extent that suspension vertical displacement is not symmetric in ride mode evaluations, roll stabilizer bar torsional windup or other auxiliary roll stiffness sources may contribute to ride rate and its asymmetry.

In the roll mode, the total axle load normal to the ground plane shall remain constant to determine the suspension characteristics resulting from a pure X_V moment. In roll mode evaluations, wheel pad X_T and Y_T forces, and Z_T moments are controlled to as near-zero as practicable. The resulting motion of the left and right contact centres define the location of the geometric roll centre. If the motion of the ground plane was constrained to roll about a fixed point, the sprung mass would be constrained to roll about that point relative to the ground plane and not free to pivot about the geometric roll centre. As a result, the measured roll stiffness would be incorrect. With a pure roll moment input to the axle, if springs with increasing rates with jounce travel are employed, for example, the wheel moving into jounce will travel less than the opposite wheel moving into rebound affecting the location of the roll centre and the roll stiffness.

For K&C measurements, ride and roll motion can be introduced by holding the wheel pads representing the ground plane fixed vertically and displacing the vehicle body in the Z_V direction or rolling it about the X_V axis. Alternatively, motions are introduced by holding the vehicle body fixed and principally displacing the wheel pads in the Z_V direction for ride mode or principally rotating them about the X_V axis for roll mode. In either case, for the roll mode the suspension roll angle shall result from a pure X_V moment and the wheel pads shall remain planar.

The gradient parameters listed below are expressed as differentials to indicate the relationship between the dependent and independent variables. However, there is no implication that any of these relationships are linear. Each cross plot of parameters will have some amount of hysteresis due to Coulomb and/or viscous friction within the suspension and steering systems. If linear coefficients are desired, it is necessary to select an operating point and determine a derivative at that point.

Dual-wheel and tyre assemblies typical of heavy trucks will be treated as a single wheel and tyre for the purposes of the following measurements.

7.2.2 Ride track change (b_z)

Ride track change, defined in ISO 8855, is the change in the distance between the tyre contact centres due to symmetric suspension ride displacement. Because the wheel pad lateral displacement is not necessarily identical to the displacement of the tyre contact centre, the track change is ideally calculated from the change in wheel centre positions and coincident inclination angles. Although track is the distance between the left and right contact centres, it is still possible to optionally determine and report the left and right contribution to ride track change separately.

7.2.3 Ride track change gradient (b_z')

Ride track change gradient, defined in ISO 8855, is calculated from the differential of the ride track change as observed in ride mode. Although track is the distance between the left and right contact

centres, it is still possible to optionally determine and report the left and right contribution to ride track change gradient separately, see Formula (11).

$$b_z' = \left(\frac{\partial b}{\partial z_{W-T}} \right) \tag{11}$$

where $z_{W\text{-}T}$ is the displacement of the wheel centres in the Z_T direction.

7.2.4 Ride steer (δ_z)

Ride steer, defined in ISO 8855, is the change in each steer angle due to symmetric suspension ride displacement.

7.2.5 Ride steer gradient (δ_z')

Ride steer gradient, defined in ISO 8855, is calculated from the differential of ride steer with suspension travel as observed in ride mode, see Formula (12).

$$\delta_z' = \left(\frac{\partial \delta}{\partial z_{W-T}} \right) \tag{12}$$

It is recommended that mean ride steer gradient be determined from an axle's mean steer angle in addition to that determined from left and right steer angle. By design, mean ride steer gradient would typically be zero. Non-zero values are indicative of the axle steering as a result of suspension heave.

7.2.6 Total ride toe ($\delta_{z(R\text{-}L)}$)

Total ride toe is the change in the difference of the left steer angle from the right steer angle observed in ride mode. The sign of total ride toe is such that the wheels are considered "toed-in" if the forward portion of the wheel is closer to the vehicle centreline than the wheel centre and "toed-out" if it is farther away. Toe-in is considered a positive angle, and toe-out is a negative angle.

7.2.7 Total ride toe gradient ($\delta_{z(R\text{-}L)}'$)

Total ride toe gradient is calculated from the differential of total ride toe with suspension travel as observed in ride mode, see Formula (13).

$$\delta_{z(R-L)}' = \left(\frac{\partial \delta_{z(R-L)}}{\partial z_{W-T}} \right) \tag{13}$$

NOTE Ride toe gradient has ramifications for tyre wear due to the change in static toe angle as a result of vehicle loading.

7.2.8 Ride camber (ε_{Vz})

Ride camber is defined in ISO 8855. It is the change in camber angle as observed in ride mode.

7.2.9 Ride camber gradient (ε_{Vz}')

Ride camber gradient, defined in ISO 8855, is calculated from the differential of ride camber with suspension travel as observed in ride mode, see Formula (14).

$$\varepsilon_{Vz}' = \left(\frac{\partial \varepsilon_V}{\partial z_{W-T}} \right) \tag{14}$$

7.2.10 Ride castor (τ_z)

Ride castor is defined in ISO 8855. It is the change in castor angle as observed in ride mode.

7.2.11 Ride castor gradient (τ_z')

Ride castor gradient, defined in ISO 8855, is calculated from the differential of ride castor with suspension travel as observed in ride mode**,** see Formula (15).

$$\tau_z' = \left(\frac{\partial \tau}{\partial z_{W-T}} \right) \tag{15}$$

7.2.12 Roll steer ($\delta_{\varphi V}$)

Roll steer, defined in ISO 8855, is the change in the left and right steer angle on an axle due to roll angle resulting from a pure X_V moment input through the tyre contact patches on an axle. In addition to the roll steer being determined for the left and right steer angle, it should also be determined for the mean steer angle.

7.2.13 Roll steer gradient ($\delta_{\varphi V}'$)

Roll steer gradient, defined in ISO 8855, is calculated from the differential of roll steer with suspension roll angle, where suspension roll angle is determined from left and right wheel centre displacements in the Z_T direction result from a pure X_V moment input through equal and opposite magnitude tyre normal forces on an axle, see Formula (16).

$$\delta_{\varphi V}' = \left(\frac{\partial \delta}{\partial \varphi_K} \right) \tag{16}$$

It is recommended that roll steer gradient be determined for an axle's mean steer angle as well as the left and right steer angle.

To the extent that chassis and suspension compliance can be neglected, roll steer gradient is directly related to ride steer gradient for independent suspensions. Steered axles with compliant steering systems will significantly alter the roll steer gradient due to the steering-axis torque resulting from the roll moment input to the suspension. For this reason, it is important to record whether the steering system was grounded at the steering wheel or the steering gear output. If the steering wheel is grounded, power assist systems shall be energized as they significantly alter steering system stiffness.

7.2.14 Roll camber ($\varepsilon_{V\varphi_V}$)

Roll camber, defined in ISO 8855, is the change in the left and right road wheel camber angle on an axle due to roll angle resulting from a pure X_V moment input through equal and opposite magnitude tyre normal forces on an axle. In addition to the roll camber being determined for the left and right road wheel camber angle, it should also be determined for the mean camber angle.

7.2.15 Roll camber gradient ($\varepsilon_{V\varphi_V}'$)

Roll camber gradient, defined in ISO 8855, is calculated from the differential of roll camber with suspension roll angle, where suspension roll angle is determined from left and right wheel centre displacements in the Z_T direction result from a pure X_V moment input through equal and opposite magnitude tyre normal forces on an axle. Roll camber gradient is one when the camber angle increases positively in direct proportion to the positive roll angle, see Formula (17).

$$\varepsilon_{V\varphi_V}' = \left(\frac{\partial \varepsilon_V}{\partial \varphi_K} \right) \tag{17}$$

7.3 Compliances

7.3.1 General

Suspension compliance characteristics are typically recorded as the linear and angular motions of the wheel centre resulting from a force in the X_T or Y_T direction, or a moment about the Z_T axis at the tyre contact centres. Wheel pad X_T and Y_T forces and Z_T moments are controlled to as near-zero as practicable (see Table 1) except for the intended force or moment input. Depending upon the metric, the wheel pads are in position control to result in no change in tyre contact centre vertical position or in force control to maintain a constant tyre vertical force.

The independent forces and moments applied to the left and right tyre contact centres are applied in the same direction or opposite directions, commonly referred to as parallel and opposed mode, respectively. Typical vehicle manoeuvres result in parallel application of *X* and *Y* forces and Z_T moments. For non-steered axles with independent suspension, compliances would typically be similar for parallel and opposed mode force and moment application with any differences primarily resulting from the non-rigid chassis. Steered axles, conversely, have very different parallel and opposed mode compliance characteristics. With parallel inputs, the compliance of the steering system results in higher, and typically more non-linear, compliance. Opposed inputs with symmetric suspension geometry and compliance, exhibit less compliance because the steering system experiences no additional force or moment that would tend to induce steer motion. Solid axles also have very different parallel and opposed mode compliance characteristics. With parallel inputs, the compliance of the lateral locating device results in higher compliance than with opposed inputs. Parallel and opposed mode suspension compliance measurements are necessary for accurate modelling of steered and solid axles.

Measurement of longitudinal braking compliance should be performed with the brakes locked. Likewise, tractive force compliance should be measured with the drivetrain locked. However, measuring longitudinal force compliance for braking force with inboard brakes or tractive force with independent suspensions, can result in excessive tyre rotation from half-shaft and drivetrain compliance. This may result in problems due to limited wheel pad travel. To address this, it is possible to measure compliance with the longitudinal force applied at the wheel centre, when appropriate.

Longitudinal force compliance can be relevant for forces applied at the tyre contact centre and/or the wheel centre. In a braking or accelerating manoeuvre, how the induced torque is reacted by the vehicle determines the effective location of the force input. The brake torque induced by outboard brakes is reacted by the suspension and the effective longitudinal force input is at the tyre contact patch. With inboard brakes, the brake torque is reacted by the sprung mass and the effective longitudinal force input is at the wheel centre. Similarly, a driven independent suspension utilizes half-shafts whose torque is reacted by the sprung mass and for that reason, the effective accelerating force is at the wheel centre. Live (i.e. driven solid) axles' drive torque is reacted by the suspension, so that the effective force input is at the ground.

The compliance parameters listed below are expressed as differentials to indicate the relationship between the dependent and independent variables. However, there is no implication that any of these relationships are linear. Each cross plot of parameters will have some amount of hysteresis due to Coulomb and/or viscous friction of the suspension and steering systems. If linear coefficients are desired, it is necessary to select an operating point and determine a derivative at that point.

7.3.2 Longitudinal force compliance, with suspension torque ($x_{\vec{F}_X}{}'$)

It is the change in the left and right wheel centre position in the *X* direction resulting from a force in the *X*-direction through the tyre contact patches on an axle. For both tyre contact patches, the z_T positions are held constant while $\vec{F}_{YT}$ and $\vec{M}_{ZT}$ are controlled to as near-zero as practicable. In addition to the

longitudinal force compliance being determined for the left and right road wheel, it should also be determined for the mean longitudinal force compliance, see Formula (18).

$$x_{\vec{F}_X}{}' = \left(\frac{\partial x_W}{\partial \vec{F}_{XT}} \right) \tag{18}$$

where x_W is the displacement of the wheel centre in the *X*-direction.

NOTE Longitudinal force compliance metrics with the force input at the tyre contact patch are denoted as "with suspension torque" because the suspension is required to react the moment about the Y_W axis resulting from the longitudinal force input. This will typically be measured with locked outboard brakes or with a locked drivetrain and a live axle.

7.3.3 Longitudinal force compliance, without suspension torque ($x_{\vec{F}_{XW}}{}'$)

It is the change in the left and right wheel centre position in the *X* direction resulting from a force in the *X*-direction through the wheel centres on an axle. For both tyre contact patches, the z_T positions are held constant while $\vec{F}_Y$ and $\vec{M}_{ZT}$ are controlled to as near-zero as practicable. In addition to the longitudinal force compliance being determined for the left and right road wheel, it should also be determined for the mean longitudinal force compliance, see Formula (19).

$$x_{\vec{F}_{XW}}{}' = 2\left(\frac{\partial x_W}{\partial \vec{F}_{XW}} \right) \tag{19}$$

where x_W is the displacement of the wheel centre in the *X* direction.

NOTE Longitudinal force compliance metrics with the force input at the wheel centre are denoted as "without suspension torque" because the suspension is not required to react the moment about the Y_W axis resulting from the longitudinal force input. This will typically be measured with locked inboard brakes or with a locked drivetrain and an independent suspension. It is also permissible to make this measurement with the brakes/drivetrain locked and the force input at the tyre contact patches, however half-shaft windup can result in contact patch longitudinal displacement exceeding the limits of the wheel pads.

7.3.4 Longitudinal force camber compliance, with suspension torque ($\varepsilon_{V\vec{F}_X}{}'$)

It is the change in the left and right road wheel camber angle on an axle resulting from a force in the *X*-direction through the tyre contact patches on an axle. For both tyre contact patches, the z_T positions are held constant while $\vec{F}_Y$ and $\vec{M}_{ZT}$ are controlled to as near-zero as practicable. In addition to the lateral force camber being determined for the left and right road wheel camber angle, it should also be determined for the mean camber angle, see Formula (20).

$$\varepsilon_{V\vec{F}_X}{}' = \left(\frac{\partial \varepsilon_V}{\partial \vec{F}_X} \right) \tag{20}$$

7.3.5 Longitudinal force camber compliance, without suspension torque ($\varepsilon_{V\vec{F}_{XW}}{}'$)

It is the change in the left and right road wheel camber angle on an axle resulting from a force in the *X*-direction through the wheel centres on an axle. For both tyre contact patches, the z_T positions are held constant while $\vec{F}_Y$ and $\vec{M}_{ZT}$ are controlled to as near-zero as practicable. In addition to the lateral force camber being determined for the left and right road wheel camber angle, it should also be determined for the mean camber angle, see Formula (21).

$$\varepsilon_{V\vec{F}_{XW}}{}' = \left(\frac{\partial \varepsilon_V}{\partial \vec{F}_{XW}} \right) \tag{21}$$

7.3.6 Longitudinal force steer compliance, with suspension torque ($\delta_{\vec{F}_X}{}'$)

It is the change in the left and right steer angle on an axle resulting from a force in the *X*-direction through the tyre contact patches on an axle. For both tyre contact patches, the z_T positions are held constant while $\vec{F}_Y$ and $\vec{M}_{ZT}$ are controlled to as near-zero as practicable. In addition to the lateral force steer being determined for the left and right steer angle, it should also be determined for the mean steer angle, see Formula (22).

$$\delta_{\vec{F}_X}{}' = \left(\frac{\partial \delta}{\partial \vec{F}_X} \right) \tag{22}$$

NOTE Inputting a longitudinal force at the tyre contact patch while constraining the contact patch vertical position would typically result in a change in vertical force at the contact patch. That can result in small vertical deflection of the wheel centre relative to the road surface due to suspension and tyre compliance, and possibly contribute to steer angle change.

7.3.7 Longitudinal force steer compliance, without suspension torque ($\delta_{\vec{F}_{XW}}{}'$)

It is the change in the left and right steer angle on an axle resulting from a force in the *X*-direction through the wheel centres on an axle. For both tyre contact patches, the z_T positions are held constant while $\vec{F}_{YT}$ and $\vec{M}_{ZT}$ are controlled to as near-zero as practicable. In addition to the lateral force steer being determined for the left and right steer angle, it should also be determined for the mean steer angle, see Formula (23).

$$\delta_{\vec{F}_{XW}}{}' = \left(\frac{\partial \delta}{\partial \vec{F}_{XW}} \right) \tag{23}$$

NOTE Inputting a longitudinal force at the wheel centre while constraining the contact patch vertical position would typically result in a change in vertical force at the contact patch. That could result in small vertical deflection of the wheel centre relative to the road surface due to suspension and tyre compliance, and possibly contribute to steer angle change.

7.3.8 Longitudinal force windup compliance, with suspension torque ($\tau_{\vec{F}_X}{}'$)

It is the change in the angular displacement of the wheel about the wheel-spin axis (Y_W) resulting from a force in the *X*-direction through the tyre contact patches on an axle. For both tyre contact patches, the z_T positions are held constant while $\vec{F}_{YT}$ and $\vec{M}_{ZT}$ are controlled to as near-zero as practicable. In addition to the longitudinal force windup compliance being determined for the left and right road wheel, it should also be determined for the mean longitudinal force windup compliance, see Formula (24).

$$\tau_{\vec{F}_X}{}' = \left(\frac{\partial \tau}{\partial \vec{F}_X} \right) \tag{24}$$

7.3.9 Longitudinal force windup compliance, without suspension torque ($\tau_{\vec{F}_{XW}}{}'$)

It is the change in the angular displacement of the wheel about the wheel-spin axis (Y_W) resulting from a force in the *X*-direction through the wheel centres on an axle. For both tyre contact patches, the z_T positions are held constant while $\vec{F}_{YT}$ and $\vec{M}_{ZT}$ are controlled to as near-zero as practicable. In addition to the longitudinal force windup compliance being determined for the left and right road wheel, it should also be determined for the mean longitudinal force windup compliance, see Formula (25).

$$\tau_{\vec{F}_{XW}}{}' = \left(\frac{\partial \tau}{\partial \vec{F}_{XW}} \right) \tag{25}$$

7.3.10 Lateral force compliance at the wheel centre ($y_{\vec{F}_{YW}}{}'$)

It is the change in the left and right wheel centre position in the *Y* direction resulting from a force in the *Y*-direction through the tyre contact patches on an axle. For both tyre contact patches, the z_T positions are held constant while $\vec{F}_{XT}$ and $\vec{M}_{ZT}$ are controlled to as near-zero as practicable, see Formula (26).

$$y_{\vec{F}_{YW}}{}' = \left(\frac{\partial y_W}{\partial \vec{F}_Y} \right) \tag{26}$$

where y_W is the displacement of the wheel centre in the *Y*-direction.

7.3.11 Lateral force compliance at the contact centre ($y_{\vec{F}_Y}{}'$)

It is the change in the left and right contact centre position in the *Y*-direction resulting from a force in the *Y*-direction through the tyre contact patches on an axle. For both tyre contact patches, the z_T positions are held constant while $\vec{F}_{XT}$ and $\vec{M}_{ZT}$ are controlled to as near-zero as practicable, see Formula (27).

$$y_{\vec{F}_Y}{}' = \left(\frac{\partial y}{\partial \vec{F}_Y} \right) \tag{27}$$

where *y* is the displacement at the contact centre in the *Y*-direction.

The lateral position of the contact centres shall be calculated based on the measured wheel centre lateral position and the change in inclination angle.

7.3.12 Lateral force camber compliance ($\varepsilon_{V\vec{F}_Y}{}'$)

It is the change in the left and right road wheel camber angle on an axle resulting from a force in the *Y*-direction through the tyre contact patches on an axle. For both tyre contact patches, the z_T positions are held constant while $\vec{F}_{XT}$ and $\vec{M}_{ZT}$ are controlled to as near-zero as practicable. In addition to the lateral force camber being determined for the left and right road wheel camber angle, it should also be determined for the mean camber angle. On steered axles, both parallel and opposed mode compliances should be measured, see Formula (28).

$$\varepsilon_{V\vec{F}_Y}{}' = \left(\frac{\partial \varepsilon_V}{\partial \vec{F}_Y} \right) \tag{28}$$

7.3.13 Lateral force steer compliance ($\delta_{\vec{F}_Y}{}'$)

It is the change in the left and right steer angle on an axle resulting from a force in the *Y*-direction through the tyre contact patches on an axle. For both tyre contact patches, the z_T positions are held constant while $\vec{F}_{XT}$ and $\vec{M}_{ZT}$ are controlled to as near-zero as practicable. In addition to the lateral force steer being determined for the left and right steer angle, it should also be determined for the mean steer angle. On steered axles, both parallel and opposed mode compliances should be measured. Parallel mode compliance characteristics may be nonlinear on steered axles with power steering as a result of nonlinear valve characteristics. In that case, both on-centre and off-centre compliances should be quantified for the parallel mode, see Formula (29).

$$\delta_{\vec{F}_Y}{}' = \left(\frac{\partial \delta}{\partial \vec{F}_Y} \right) \tag{29}$$

7.3.14 Aligning moment camber compliance ($\varepsilon_{V\vec{M}_Z}{}'$)

It is the change in the left and right road wheel camber angle on an axle resulting from a pure moment about the Z_T axis through the tyre contact patches on an axle. For both tyre contact patches, the Z_T positions are held constant while $\vec{F}_{XT}$ and $\vec{F}_{YT}$ are controlled to as near-zero as practicable. In addition to the aligning moment camber being determined for the left and right road wheel camber angle, it should also be determined for the mean camber angle. On steered axles, both parallel and opposed mode compliances should be measured, see Formula (30).

$$\varepsilon_{V\vec{M}_Z}{}' = \left(\frac{\partial \varepsilon_V}{\partial \vec{M}_{ZT}} \right) \tag{30}$$

7.3.15 Aligning moment steer compliance ($\delta_{\vec{M}_Z}{}'$)

It is the change in the left and right steer angle on an axle resulting from a pure moment about the Z_T axis through the tyre contact patches on an axle. For both tyre contact patches, the z_T positions are held constant while $\vec{F}_{XT}$ and $\vec{F}_{YT}$ are controlled to as near-zero as practicable. In addition to the aligning moment steer being determined for the left and right steer angle, it should also be determined for the mean steer angle. On steered axles, both parallel and opposed mode compliances should be measured. Parallel mode compliance characteristics can be significantly nonlinear on steered axles with power steering as a result of nonlinear valve characteristics. In that case, both on-centre and off-centre compliances should be quantified for the parallel mode, see Formula (31).

$$\delta_{\vec{M}_Z}{}' = \left(\frac{\partial \delta}{\partial \vec{M}_{ZT}} \right) \tag{31}$$

7.4 Ride and roll stiffness

7.4.1 General

The rate and stiffness parameters listed below are expressed as differentials to indicate the relationship between the dependent and independent variables. However, there is no implication that any of these relationships are linear. Each cross plot of parameters will have some amount of hysteresis due to Coulomb and/or viscous friction of the suspension and steering systems. If linear coefficients are desired, it is necessary to decide upon an operating point and determine a derivative at that point.

Special consideration should be taken for axles with inter-connected pneumatic or hydraulic springs, and for axles with ride height control valves. During a dynamic cornering event, the effects of spring fluid pressure transfer across an axle as a result of roll angle are limited by the short duration of the manoeuvre. During a ride or pitching event, the effects of spring pressure change as a result of a ride height control valve are similarly limited by the short duration of the event. During quasi-static K&C measurements, inter-axle pressure transfer and ride height control valve pressure adjustments have a drastic effect on measurements. The pressure supply to the springs or accumulators may need to be blocked with a manual valve after establishing the operational trim of the vehicle. Any modification that is necessary for the K&C test shall be described and included with the results.

7.4.2 Ride rate (K_Z)

Ride rate, defined in ISO 8855, is the rate of change of the force in the Z_T-direction into the tyre contact patch with respect to the change in the left and right tyre contact centre or wheel pad z_T-position. For both tyre contact patches, the z-positions are position-controlled while $\vec{F}_{XT}$, $\vec{F}_{YT}$, and $\vec{M}_{ZT}$ are

controlled to as near-zero as practicable. In addition to the ride rate being determined for the left and right road wheel, it should also be determined for the mean ride rate, see Formula (32).

$$K_Z = \left(\frac{\partial \vec{F}_{ZT}}{\partial z_T} \right) \tag{32}$$

where z_T is the displacement of the tyre contact centre in the Z_T-direction.

NOTE Ideally, the ride rate measurement is conducted in force control such that only the original static roll moment is applied to the axle. However, typically the wheel pads are in displacement control such that the left and right wheel pads experience equal vertical displacement. In most cases, this is not a concern unless there is a vertical load transferred between the left and right suspensions with symmetric vertical displacement. This can occur, for example, in suspensions with interconnected air springs.

7.4.3 Suspension ride rate (K_{ZK})

Suspension ride rate, defined in ISO 8855, is the rate of change of the force in the Z_T-direction into the tyre contact patch with respect to the change in the left and right wheel centre z_W-position. For both tyre contact patches, the z_T positions are position-controlled while $\vec{F}_{XT}$, $\vec{F}_{YT}$, and $\vec{M}_{ZT}$ are controlled to as near-zero as practicable. In addition to the suspension ride rate being determined for the left and right road wheel, it should also be determined for the mean suspension ride rate, see Formula (33).

$$K_{ZK} = \left(\frac{\partial \vec{F}_{ZT}}{\partial z_{W-T} \cdot \cos(\varepsilon_V)} \right) \tag{33}$$

where $z_{W\text{-}T}$ is the displacement of the wheel centres in the Z_T-direction. Also, see NOTE in 7.4.2.

7.4.4 Roll stiffness (K_{φ_V})

Roll stiffness, defined in ISO 8855, is calculated from the differential of vehicle roll moment with roll angle, where roll angle is determined from left and right contact centre displacements in the Z_T-direction resulting from a pure X_V moment input through equal and opposite magnitude tyre normal forces on an axle. The left and right tyre contact patches on each axle shall remain in the same plane, see Formula (34).

$$K_{\varphi_V} = \left(\frac{\partial \vec{M}_X}{\partial \varphi_V} \right) \tag{34}$$

where roll moment is determined from Formula (35):

$$\vec{M}_X = b \cdot (\vec{F}_{ZT(R)} - \vec{F}_{ZT(L)}) \tag{34}$$

and roll angle may be determined from Formula (35):

$$\varphi_V = \frac{180/\pi}{b} \cdot (z_{T(R)} - z_{T(L)}) \tag{35}$$

7.4.5 Suspension roll stiffness (K_{φ_K})

Suspension roll stiffness, defined in ISO 8855, is calculated from the differential of vehicle roll moment with suspension roll angle, where suspension roll angle is determined from left and right wheel centre displacements in the Z_T direction resulting from a pure X_V moment input through equal and opposite

magnitude tyre normal forces on an axle. The left and right tyre contact patches on each axle shall remain in the same plane, see Formula (36).

$$K_{\varphi_K} = \left(\frac{\partial \vec{M}_X}{\partial \varphi_K} \right) \tag{36}$$

where suspension roll angle may be determined from Formula (37):

$$\varphi_K = \frac{180/\pi}{b} \cdot \left[z_{W(R)} \cdot \cos\left(\varepsilon_{V(R)}\right) - z_{W(L)} \cdot \cos\left(\varepsilon_{V(L)}\right) \right] \tag{37}$$

7.4.6 Auxiliary roll stiffness ($K_{\varphi_V,\text{aux}}$)

It is the difference in the measured roll stiffness for an axle and the roll stiffness contribution that results from the factors that produce ride rate, see Formula (38).

$$K_{\varphi_V,\text{aux}} = K_{\varphi_V} - K_{\varphi_V Z} \tag{38}$$

where $K_{\varphi_V Z}$ is the roll stiffness contribution resulting from only the factors that produce ride rate, see Formulae (39) and (40).

For independent suspensions: $K_{\varphi_V Z} = \frac{1}{2} \cdot K_Z \cdot b^2$ (39)

For solid axles: $K_{\varphi_V Z} = \frac{1}{2} \cdot K_Z \cdot s^2$ (40)

where b is the track and s is the spacing between the spring centres in the Y_V direction.

7.4.7 Auxiliary suspension roll stiffness ($K_{\varphi_K,\text{aux}}$)

It is the difference in the measured suspension roll stiffness for an axle and the roll stiffness contribution that results from the factors that produce suspension ride rate, see Formula (41).

$$K_{\varphi_K,\text{aux}} = K_{\varphi_K} - K_{\varphi_K Z} \tag{41}$$

where $K_{\varphi_K Z}$ is the suspension roll stiffness contribution resulting from only the factors that produce suspension ride rate, see Formulae (42) and (43).

For independent suspensions: $K_{\varphi_K Z} = \frac{1}{2} \cdot K_{ZK} \cdot b^2$ (42)

For solid axles: $K_{\varphi_K Z} = \frac{1}{2} \cdot K_{ZK} \cdot s^2$ (43)

where b is the track and s is the spacing between the spring centres in the Y_V direction.

7.4.8 Vertical displacement tandem axle load redistribution stiffness (K_{tz})

It is the rate of redistribution of total axle load from one axle of a tandem to the other with respect to equal and opposite axle tyre contact centre displacement in the Z_T-direction, see Formula (44).

$$K_{tz}' = \left(\frac{\partial \vec{F}_{Z(F-R)}}{\partial z_{(F-R)}} \right) \tag{44}$$

NOTE The forces and displacements are measured and imparted from the wheel pad.

7.4.9 Vertical suspension displacement tandem axle load redistribution stiffness (K_{tzK})

It is the rate of redistribution of total axle load from one axle of a tandem to the other with respect to equal and opposite axle wheel centre displacement in the Z_T-direction, see Formula (45).

$$K_{tzK}{}' = \left(\frac{\partial \vec{F}_{Z(F\text{-}R)}}{\partial zw_{(F\text{-}R)}} \right) \tag{45}$$

NOTE The forces are measured and imparted from the wheel pad. The displacements are measured from the wheel centre.

7.4.10 Tandem axle twist stiffness ($K_{\varphi t}$)

It is the combined roll stiffness (K_φ) of a tandem axle pair with the roll angle of each axle controlled to equal and opposite values. The roll angle is determined from left and right contact centre displacements in the Z_T direction resulting from a pure X_V moment input through equal and opposite magnitude tyre normal forces on an axle. The left and right tyre contact patches on each axle shall remain in the same plane. The signs of roll moment and roll angle are such that subtracting those of the rear axle from those of the front axle results in a summation of magnitudes, see Formula (46).

$$K_{\varphi t} = \left(\frac{\partial \vec{M}_{X(F\text{-}R)}}{\partial \varphi_{(F-R)}} \right) \tag{46}$$

7.4.11 Tandem axle suspension twist stiffness ($K_{\varphi tK}$)

It is the combined suspension roll stiffness (K_{φ_K}) of a tandem axle pair with the suspension roll angle of each axle controlled to equal and opposite values. The suspension roll angle is determined from left and right wheel centre displacements in the Z_T direction resulting from a pure X_V moment input through equal and opposite magnitude tyre normal forces on an axle. The left and right tyre contact patches on each axle shall remain in the same plane. The signs of roll moment and suspension roll angle are such that subtracting those of the rear axle from those of the front axle results in a summation of magnitudes, see Formula (47).

$$K_{\varphi tK} = \left(\frac{\partial \vec{M}_{X(F\text{-}R)}}{\partial \varphi_{K(F-R)}} \right) \tag{47}$$

7.4.12 Tyre normal stiffness (K_{ZT})

Defined in ISO 8855, the left and right tyre normal stiffness can be determined from left and right ride rate and suspension ride rate measurements as in Formula (48):

$$K_{ZT} = \frac{K_{ZK} \cdot K_Z}{K_{ZK} + K_Z} \tag{48}$$

7.5 Force reactions

7.5.1 Anti-squat and anti-dive force gradient ($\vec{F}_{Z\vec{F}_X}{}'$)

The change in $\vec{F}_{ZT}$ resulting from a pure $\vec{F}_{XT}$ force. Anti-squat and anti-dive force gradient can be calculated from data measured during the longitudinal force compliance test if $\vec{F}_{ZT}$ is recorded. The contact centre z_T positions are position-controlled and $\vec{F}_{YT}$ and $\vec{M}_{ZT}$ are controlled to as near-zero as

practicable. According to this sign convention, anti-squat force reaction will have a positive gradient and anti-dive force reaction will have a negative gradient, see Formula (49).

$$\vec{F}_{Z\vec{F}_X}{}' = \left(\frac{\partial \vec{F}_{ZT}}{\partial \vec{F}_{XT}} \right) \tag{49}$$

7.5.2 Jacking force gradient ($\vec{F}_{Z\vec{F}_Y}{}'$)

It is the change in $\vec{F}_{ZT}$ resulting from a pure $\vec{F}_{YT}$ force. Jacking force gradient can be calculated from data measured during the lateral force compliance test if $\vec{F}_{ZT}$ is recorded. The contact centre z_T positions are position-controlled and $\vec{F}_{XT}$ and $\vec{M}_{ZT}$ are controlled to as near-zero as practicable, see Formula (50).

$$\vec{F}_{Z\vec{F}_Y}{}' = \left(\frac{\partial \vec{F}_{ZT}}{\partial \vec{F}_{YT}} \right) \tag{50}$$

7.5.3 Longitudinal force tandem axle load redistribution gradient ($W_{Dt\vec{F}_{XT}}{}'$)

It is the redistribution of total axle load from one axle of a tandem to the other with respect to a longitudinal force in the X_T-direction imparted equally to all tyres in the tandem, see Formula (51).

$$W_{Dt\vec{F}_{XT}}{}' = \left(\frac{\partial \vec{F}_{Z(F\text{-}R)}}{\partial \vec{F}_{XT}} \right) \tag{51}$$

8 Data presentation

8.1 Steering ratio

Steering ratio data may be presented as a plot of the steering angle measured at each road wheel versus the steering wheel angle measured at the hand wheel, as shown in Figure 2. The steering ratio and characteristic model(s) shall be presented as a function of steering hand wheel angle, as shown in Figure 3. Ackerman error and turning radius may also be presented, as shown in Figure 4.

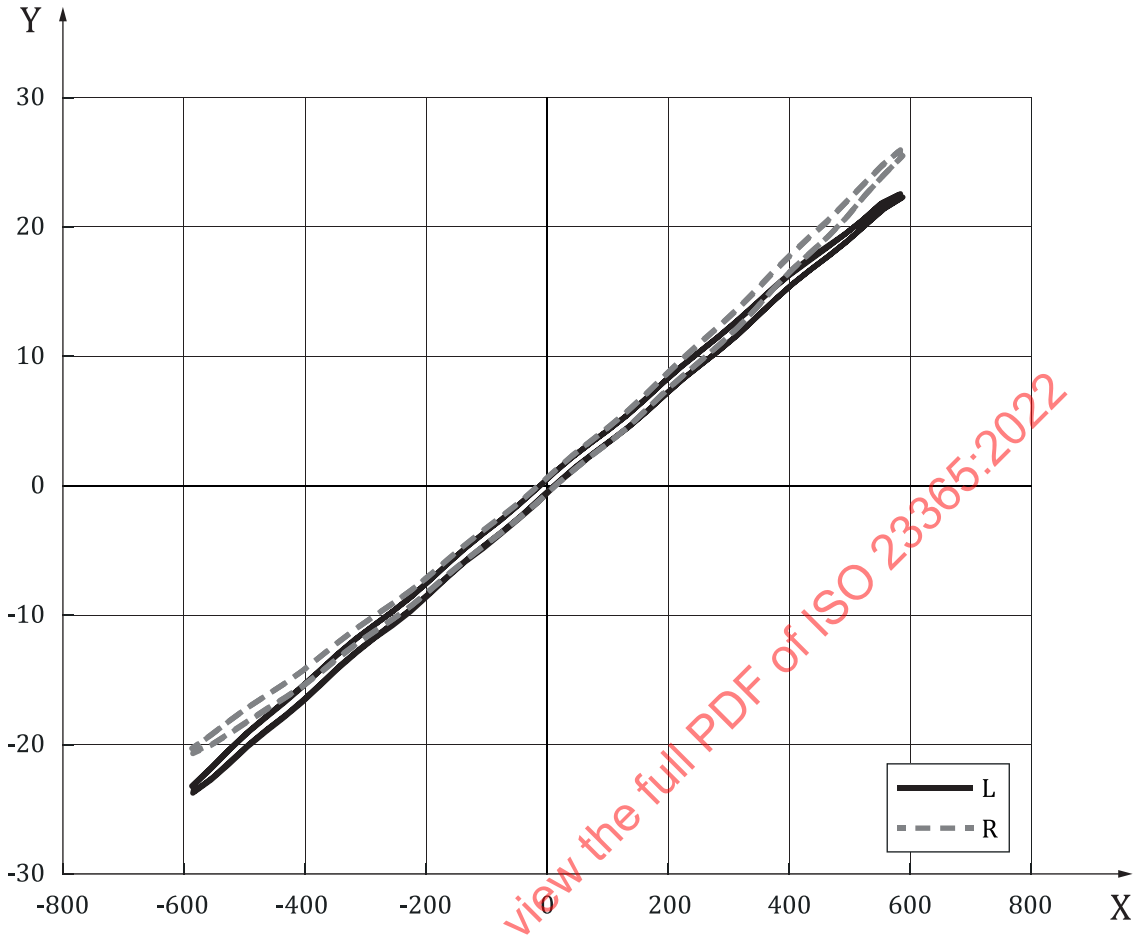

Key

X steering hand wheel angle, [°]
Y road wheel steering angle, [°]
L left road wheel
R right road wheel

Figure 2 — Left and right steer angle versus steering-wheel angle